Original Investigation

MRI-Based Classification for Tibial Spine Fracture: Detection Efficacy, Classification Accuracy, and Reliability

Rania Mostafa Almolla, Yassir Edrees Almalki, Mohammad Abd Alkhalik Basha,[1], Mohamed Abd El-Aziz Mohamed Farag, Maha Ibrahim Metwally, Mohamad Gamal Nada, Yasmin Ibrahim Libda, Mohamed M.A. Zaitoun, Ahmed A. El-Hamid M. Abdalla, Hala Y. Yousef, Marwa E. Abd Elhamed, Amgad M. Elsheikh, Sharifa Khalid Alduraibi, Diaa Bakry Eldib, Hamada M. Khater, MD, Hossam Fathi Mahmoud, Engy S. Elkayal, Shaker Hassan S. Alshehri, Asim S. Aldhilan, Ahmed M.A. Basha, Hanan A. Hassan

Rationale and Objectives: Recently, a new MRI-based classification for evaluating tibial spine fractures (TSFs) was developed to aid in treating these injuries. Our objective was to assess the detection efficacy, classification accuracy, and reliability of this classification in detecting and grading TSFs, as well as its impact on treatment strategy, compared to the Meyers and McKeever (MM) classification.

Materials and Methods: A retrospective study included 68 patients with arthroscopically confirmed TSFs. All patients had plain radiography and conventional MRI of the affected knee before arthroscopy. Three experienced radiologists independently reviewed all plain radiographs and MRI data and graded each patient according to MM and MRI-based classifications. The detection efficacy, classification accuracy, and inter-rater agreement of both classifications were evaluated and compared, using arthroscopic findings as the gold standard.

Results: The final analysis included 68 affected knees. Compared to the MM classification, the MRI-based classification produced 22.0% upgrade of TSFs and 11.8% downgrade of TSFs. According to the reviewers, the fracture classification accuracy of the MRI-based classification (91.2–95.6%) was significantly higher than that of the MM classification (73.5–76.5%, $p = 0.002–0.01$). The fracture detection rate of MRI-based classification (94.1–98.5%) was non-significantly higher than that of the MM classification (83.8–89.7%, $p = 0.07–0.4$). The soft tissue injury detection accuracy for MRI-based classification was 91.2–94.1%. The inter-rater reliability for grading TSFs was substantial for both the MM classification ($\kappa = 0.69$) and MRI-based classification ($\kappa = 0.79$).

Conclusion: MRI-based classification demonstrates greater accuracy and reliability compared to MM classification for detecting and grading TSFs and associated soft tissue injuries.

Key Words: Knee; Tibial spine fractures; Mayer and McKeever classification; MRI.

Acad Radiol 2024; 31:1480–1490

From the Department of Radio-diagnosis, Faculty of Human Medicine, Zagazig University, Zagazig, Egypt (R.M.A., M.A.A.B., M.I.M., M.G.N., Y.I.L., M.M.A.Z., A.A.E-H.M.A., H.Y.Y., M.E.A.E., A.M.E., H.A.H.); Division of Radiology, Department of Internal Medicine, Medical College, Najran University, Najran, Kingdom of Saudi Arabia (Y.E.A.); Department of Radio-diagnosis, Faculty of Human Medicine, Al Azhar University, Cairo, Egypt (M.A.E-A.M.F.); Department of Radiology, College of Medicine, Qassim University, Buraidah, Kingdom of Saudi Arabia (S.K.A., A.S.A.); Department of Radio-diagnosis, Faculty of Human Medicine, Benha University, Benha, Egypt (D.B.E., H.M.K.); Department of Orthopedic Surgery and Traumatology, Faculty of Human Medicine, Zagazig University, Zagazig, Egypt (H.F.M.); Department of Radio-diagnosis, Faculty of Human Medicine, Fayoum University, Fayoum, Egypt (E.S.E.); Department of Orthopedic Surgery, College of Medicine, King Khalid University, Abha, Kingdom of Saudi Arabia (S.H.S.A.); Faculty of General Medicine, Tyumen State Medical University, Tyumen, Russian Federation (A.M.A.B.). Received September 4, 2023; revised October 2, 2023; accepted October 3, 2023. **Address correspondence to**: M.A.A.B. e-mail: Mohammad_basha76@yahoo.com

[1] ORCID iD: 0000-0002-9075-8020

https://doi.org/10.1016/j.acra.2023.10.007

INTRODUCTION

Tibial spine fractures (TSFs) are avulsion fractures of the anterior cruciate ligament (ACL) from its attachment to the tibial condylar eminence, representing 2–5% of all pediatric knee injuries (1–3). TSFs can occur in adults; however, children and adolescents with immature skeletons (8–14 years) are more susceptible to this fracture (4,5). Treatment can be non-operative or operative, depending on the type and displacement of fracture. However, the optimal management remains controversial, with conflicting data regarding the best approach (6,7).

It is crucial for radiologists to accurately identify TSFs, as failure or delay in diagnosis can lead to non-union and persistent clinical symptoms, such as limitation or pain in knee extension and anterior instability (8). The initial diagnosis of TSFs is primarily based on plain radiographs (3,9). However, small, avulsed fragments can be difficult to recognize on radiographs, leading to potential misdiagnosis (10). Computed tomography (CT) better characterizes bony fragments and fracture extension. However, magnetic resonance imaging (MRI) has become the imaging modality of choice for assessing and confirming these injuries, as it allows for high-quality visualization of fracture displacement, concomitant injuries, and potential ACL involvement (3,9,10).

There are several classifications for grading TSFs. The oldest and most commonly used classification was developed in 1959 by Meyers and McKeever (MM) (11). The MM described three types of fractures based on the degree of displacement of the fractured fragment: Type I (non-displaced fragment), type II (partially displaced or hinged fragment), and type III (completely displaced fragment). In 1970, MM further subdivided type III fractures into non-rotated and rotated ones (12). In 1977, Zaricznyj (13) described a fourth type of fracture that included complete displacement and comminution. These older classifications were designed for use with plain radiographs; however, an increasing number of physicians are now evaluating TSFs using MRI (14–16). In 2019, Green et al. (17) developed a new MRI-based classification for TSFs. This MRI-based classification categorizes TSFs into three grades according to specific quantitative assessments of fracture size and pattern, fragment displacement, and soft tissue involvement. Green et al. (17) recommended that MRI should be routinely performed for patients with TSFs, as the use of the MRI-based classification reduces ambiguity in grading and has the potential to streamline treatment decisions. However, despite the wide use of MRI, most patients are still treated without pre-treatment MRI (18). Moreover, no studies have assessed the recent MRI-based classification designed by Green et al. (17). Therefore, we conducted a retrospective study to assess the detection efficacy, classification accuracy, and reliability of this MRI-based classification for detecting and grading TSFs. We also compared it to the MM classification in terms of impact on treatment strategies.

MATERIALS AND METHODS

Patient Population

The clinical data of patients in our institution with arthroscopically proved TSFs between January 1, 2018, and June 30, 2023, were retrospectively evaluated. Inclusion criteria were as follows (i) arthroscopically confirmed TSFs, and (ii) plain radiography and MRI of the affected knee at our institution, with standardized protocols. Patients with chronic knee disorders (n = 13), multiple trauma (n = 11), open fractures, or emergency surgery (n = 10) were excluded from the study. Initially, 102 patients were included in the study. Based on exclusion criteria, 68 patients (males, 47; females, 21; mean age, 16.8 ± 3.2 years; range, 7–39 years) were included in the final cohort. The flowchart of the study is illustrated in Figure 1. The methods of injury included sport-related injuries in 28 patients, traffic accidents in 25, and falls from a height in 15. All patients underwent MRI examinations within 11–19 days after injury (mean, 13.2 ± 3.7 days). 40 patients underwent arthroscopy with internal fixation (ARIF), and 28 underwent open reduction and internal fixation (ORIF). Patients' demographic data are presented in Table 1.

Plain Radiography Protocol

Two standard X-ray views were obtained. Anteroposterior (AP) view: the patient lay supine with the knee and ankle joint in contact with the table, and the leg was extended. The X-ray beam was directed from the front to the back of the knee joint. The central ray was directed to the center of the knee at a point 1.3 cm inferior to the patellar apex, parallel to the articular facets. This view showed the tibial spine and its alignment in relation to the tibia and femur. Lateral view: the patient lay on the affected side with the affected knee closest to the table and the other lower limb flexed anteriorly. The affected knee was slightly flexed by approximately 30° (to the best of the patient's ability). The X-ray beam was directed perpendicular to the knee joint from the side. The central ray was directed to the center of the knee at a point 1.3 cm inferior to the patellar apex. This view provided additional information regarding the fracture pattern, displacement, and potentially associated injuries. The following settings were used: 60–80 kVp, 10–20 mA, 100 cm image-receptor distance, and 0.05 s exposure time. Pediatric radiology protocol with the lowest radiation dose that allowed for adequate image quality was used for pediatric patients. This included adjusting settings such as kVp and mA, as well as adjusting beam filtration.

MRI Protocol

All MRI examinations were conducted in the same week as the plain radiographs. MRI examinations were performed on a 1.5-T (Achieva, Philips Medical System, Eindhoven, Netherlands) using a phased-array knee coil with an internal

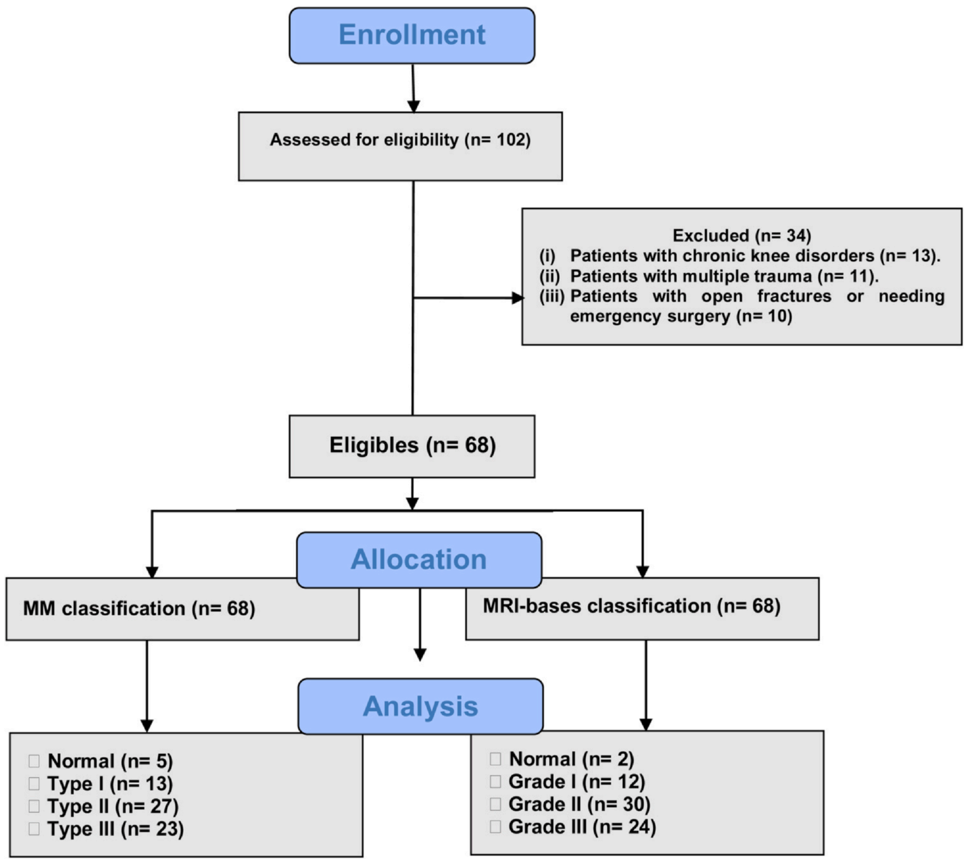

Figure 1. Flowchart of the study.

diameter of 28 mm. Coronal, sagittal, and axial two-dimensional (2D) T1-weighted (T1W) fast spin-echo (FSE) imaging (TR/TE:500/8); coronal and sagittal 2D T2W FSE imaging (TR/TE= 5000/45); coronal and sagittal proton density-weighted (PDW) FSE imaging (TR/TE= 2000/40); and coronal T2W-short tau inversion recovery (STIR) were obtained for all patients. Field-of-view was 160 × 160 mm, slice thickness was 4 mm, inter-gap spacing was 0.8 mm, and matrix was 192 × 256. Optimized sequences to minimize scan time and the need for sedation were used in pediatric patients. Pediatric specialists were requested to provide sedation and monitor patients closely throughout the MRI in a few patients.

TABLE 1. Patients' Data

Variable	Value
Age, years, mean ± SD (range)	16.8 ± 3.2 (7–39)
Sex	
Male	47 (69.1)
Female	21 (30.9)
Laterality	
Right	39 (57.4)
Left	29 (42.6)
Methods of injury	
Sport-related injuries	28 (41.2)
Traffic accidents	25 (36.8)
Falls from height	15 (22)
Period between injury and MRI, days, mean ± SD (range)	13.2 ± 3.7 (11–19)
Treatment	
ARIF	40 (39.2)
ORIF	28 (27.5)

Unless otherwise indicated, the data are represented as numbers with the corresponding percentages in parentheses. ARIF, arthroscopy with internal fixation; MRI, magnetic resonance imaging; ORIF, open reduction and internal fixation; SD, standard deviation.

Image Analysis

All plain radiographs and MRI images were centrally viewed on a Picture Archiving and Communication System (PACS). Three radiologists (BLINDED, with 10, 14, and 19 years of experience in musculoskeletal imaging, respectively) retrospectively and independently reviewed all images. Discrepancies in interpretation were resolved by consensus. The radiologists were blinded to the clinical information and arthroscopic reports. Plain radiographs and MR images were reviewed separately (i.e., plain image findings were reviewed without knowledge of MRI findings). Initially, the three radiologists reviewed the plain radiographs. They reported the presence or absence of the fracture line, displaced fragment, distance of displacement, and anterior and posterior

TABLE 2. Types and Grades of TSF Stratified by Classification and Reviewer

Type	R1	R2	R3	Consensus Reviewing
MM classification				
Normal	5 (7.4)	11 (16.2)	8 (11.8)	5 (7.4)
Type I	12 (17.6)	18 (26.5)	21 (30.9)	13 (19.1)
Type II	24 (35.3)	20 (29.4)	19 (27.9)	27 (39.7)
Type III	27 (39.7)	19 (27.9)	20 (29.4)	23 (33.8)
MRI-based classification				
Normal	3 (4.4)	2 (2.9)	1 (1.5)	2 (2.9)
Grade I	8 (11.8)	19 (27.9)	15 (22.0)	12 (17.6)
Grade II	26 (38.2)	19 (27.9)	38 (55.9)	30 (44.1)
Grade III	31 (45.6)	28 (41.2)	14 (20.6)	24 (35.3)

The data are represented as numbers with the corresponding percentages in parentheses. MM, Meyers and McKeever; MRI, magnetic resonance imaging; R, radiologist; TSFs; Tibial spine fractures.

ends of the displaced fragment. Finally, they classified each patient into three main types using the MM classification (11):

- Type I: Non-displaced fragment.
- Type II: Displaced anterior margin and hinged posterior cortex of the fragment.
- Type III: Complete separation of the fragment.

After one month, the same three radiologists independently reviewed all MR images to reduce memory bias. They reported the presence or absence of displacement in the tibial eminence, measured the anterior and posterior displacement of the hinged fragment, and reported the associated soft tissue injury as an ACL tear (partial or complete), meniscal entrapment or tear, osteochondral injury, or collateral ligament injury. Finally, they classified each patient into three grades based on the new MRI-based classification system developed by Green et al. (17):

- Grade I: Non or minimally displaced fractures (≤2 mm displacement).
- Grade II: Posterior-hinged fractures (> 2 mm displacement of the anterior aspect of the fragment or ≤2 mm displacement of the posterior aspect of the fragment).
- Grade III: Displaced fractures (> 2 mm displacement of the posterior aspect of the fragment), fractures with meniscal or inter-meniscal ligament entrapment, or fractures extending to the articular surface of the medial or lateral tibial plateau with > 2 mm displacement.

Reference Standard

Based on the orthopedic surgeon's decision, 40 patients underwent ARIF, and 28 underwent ORIF using a tight rope system for fragment fixation. The surgical treatment of associated soft tissue injuries was documented. Arthroscopic reports were retrospectively evaluated for the grade of the TSFs and associated soft tissue injuries. The operative data at the time of arthroscopy were compared to those predicted using preoperative plain radiography and MRI.

Statistical Analysis

The collected data were computerized and statistically analyzed using MedcCalc version 15.8 (Mariakerke, Belgium) and SPSS version 26 (IBM, Armonk, NY, USA). Qualitative data were represented as frequencies and relative percentages, and the Chi-square test was used for comparison. Fracture classification accuracy was determined using the four-fold table. The intraclass correlation coefficient (ICC) and kappa statistics with 95% confidence intervals (CIs) were used to assess the interrater and intermodality agreement. The κ values were interpreted as follows: < 0.2 indicates poor agreement, 0.21–0.4 indicates fair agreement, 0.41–0.6 indicates moderate agreement, 0.61–0.8 indicates substantial agreement and 0.81–1.00 indicates perfect agreement. Statistical significance was set at $P < 0.05$.

RESULTS

Assignment of TSF Type and Grade According to Both Classifications

The types and grades of TSFs, stratified by classification and reviewers are detailed in Table 2.

Grade Changes Between Both Classifications

The change in individual TSF grading due to the application of MRI-based classification, compared to the MM classification, is presented in Table 3. In comparison to MM classification, MRI-based classification resulted in 22.0% (15/68) upgrade of the TSFs [5.9% (4/68) normal, 10.3% (7/68) in type I, and 5.9% (4/68) in type II], and 11.8% (8/68) downgrade of the TSFs [1.5% (1/68) in type I, 4.4% (3/68) in type II, and 5.9% (4/68) in type III]. Therefore, the MRI-based classification changed the treatment plan for 33.8% of the patients.

TABLE 3. Change in Individual TSF Grading on Account of MRI-Based Classification, Compared to MM Classification, According to Consensus Reviewing

MRI-Based classification	MM classification				
	Normal	Type 1	Type II	Type III	Total
Normal	1 (1.5)	1 (1.5)			2 (2.9)
Grade I	4 (5.9)	5 (7.4)	3 (4.4)	0	12 (17.6)
Grade II	0	6 (8.8)	20 (29.4)	4 (5.9)	30 (44.1)
Grade III	0	1 (1.5)	4 (5.9)	19 (27.9)	24 (35.3)
Total	5 (7.4)	13 (19.1)	27 (39.7)	23 (33.8)	68 (100)

The data are represented as numbers with the corresponding percentages in parentheses. MM, Meyers and McKeever; MRI, magnetic resonance imaging; TSFs; Tibial spine fractures. The different colors indicate whether MRI-based classification upgraded (green), downgraded (blue) or kept the grade the same (yellow) as MM Classification.

Associated Soft Tissue Injuries

Table 4 presents the associated soft tissue injuries detected by MRI compared to the arthroscopic results. There was perfect agreement between MRI and arthroscopy for detecting associated soft tissue injuries ($\kappa = 0.85$).

Detection Efficacy and Classification Accuracy of Both Classifications

Among the 68 operated patients, 59–61 patients on plain radiographs and 64–67 patients on MRI exhibited TSFs, according to the radiologist. The fracture detection rate was 83.8–89.7% for the MM classification and 94.1–98.5% for the MRI-based classification. Out of the 68 patients, 51–52 patients on plain radiographs and 62–65 on MRI showed accurate grading of TSFs, according to the radiologist. The fracture classification accuracy was 73.5–76.5% for MM classification and 91.2–95.6% for MRI-based classification. The soft tissue injury detection accuracy for MRI-based classification ranged from 91.2% to 94.1%. The MRI-based classification had significantly higher classification accuracy than the MM classification ($p = 0.002$–0.01). The fracture detection rate and classification accuracy of both classifications are summarized in Table 5.

Interrater and Intermodality Agreement

The inter-rater reliability for grading TSFs was substantial for both the MM classification ($\kappa = 0.69$; 95% CI = 0.60–0.76), and MRI-based classification ($\kappa = 0.79$; 95% CI = 0.73–0.85). There was a substantial agreement between MM classification and MRI-based classification regarding the grading of TSFs

TABLE 4. Associated Soft Tissue Injury by MRI Compared to Arthroscopic Results and Their Agreement, According to Consensus Reviewing

Associated Injury	MRI-Based Classification	Surgical Results	κ-Agreement
Meniscal entrapment			0.85
Medial meniscus	7 (10.3)	4 (5.9)	Perfect agreement
Transverse meniscal ligament	2 (2.9)	2 (2.9)	
Meniscal tear			
Medial	29 (42.6)	33 (48.5)	
Lateral	18 (26.5)	15 (22.1)	
ACL			
Partial tear	20 (29.4)	24 (35.3)	
Complete tear	35 (51.5)	40 (58.8)	
Collateral ligaments			
LCL	18 (26.5)	15 (22.1)	
MCL	22 (32.4)	26 (38.2)	
Chondral injury	53 (77.9)	53 (77.9)	

The data are represented as numbers with the corresponding percentages in parentheses. ACL, anterior cruciate ligament; LCL, lateral collateral ligament; MCL, medial collateral ligament; MRI, magnetic resonance imaging.

TABLE 5. Fracture Detection Rate and Classification Accuracy of MM and MRI-Based Classifications Using Arthroscopic Data as the Gold Standard

	MM Classification			MRI-Based Classification			P-value
	R1	R2	R3	R1	R2	R3	
Fracture detection rate	88.2 (60/68)	83.8 (57/68)	89.7 (61/68)	94.1 (64/68)	95.6 (65/68)	98.5 (67/68)	0.07–0.4
Fracture classification accuracy	73.5 (50/68) [61.4–83.5]	76.5 (52/68) [64.6–85.9]	75.1 (51/68) [63.0–84.7]	91.2 (62/68) [81.8–96.7]	94.1 (64/68) [85.6–98.4]	95.6 (65/68) [87.6–99.1]	0.002–0.01
Soft tissue injury detection accuracy	-	-	-	91.2 (62/68) [81.8–96.7]	89.7 (61/68) [79.9–95.8]	94.1 (64/68) [85.6–98.4]	-

Data in parentheses were used to calculate percentages. Data in brackets are 95% confidence intervals. MM, Meyers and McKeever; MRI, magnetic resonance imaging; R, radiologist.

($\kappa = 0.69$; 95% CI = 0.57–0.81). When compared to arthroscopic results in 68 operated patients, a perfect agreement was found with the MRI-based classification ($\kappa = 0.91$; 95% CI =0.84–0.99), and substantial agreement with the MM classification ($\kappa = 0.77$; 95% CI = 0.55–0.81). Representative cases from our study are shown in Figs. 2-4.

DISCUSSION

Despite the widespread use of MRI, the level of evidence for MRI and the new MRI-based classification of TSFs is limited in the current literature. Therefore, the present study was conducted on 68 patients with arthroscopically proven TSFs to evaluate the detection efficacy, classification accuracy, and reliability of this new MRI-based classification. The overall results are encouraging and confirming the high detection efficacy and reliability of this new classification and highlight its promising potential as a diagnostic tool for accurately grading TSFs. Our study demonstrated that MRI-based classification provided higher detection efficacy (94.1–98.5%) and classification accuracy (91.2–95.6%) for detecting and grading TSFs compared to MM classification, which had lower detection efficacy (83.8–89.7%) and classification accuracy (73.5–76.5%). This finding is not surprising, considering that it relies on MRI, which has been proven in previous studies to be an accurate and reliable imaging technique for evaluating TSFs (5,18–21).

The use of MRI-based classification has the potential to cause grading discrepancies; thus, it is important to investigate how these grade changes truly impact the classification of TSFs and the final grading outcomes of the MRI-based classification. Our results showed that the MRI-based classification led to a significant change in grading for 33.8% of patients, with an upgrade in 22.0% of patients and a downgrade in 11.8% of patients, compared to the MM classification. These results indicate that the MRI-based classification altered the treatment recommendations in 33.8% of our patients, which aligns with the findings of Green et al. (17), who found that the MRI-based classification changed the TSF grade in 32.5% of patients.

In our study, four patients were missed on plain radiographs and diagnosed by MRI as having TSF grade I. This underscores the role of MRI in identifying even non-displaced fractures. Thin fracture lines with surrounding edema can be easily overlooked on plain radiographs during the acute stage. In fact, these four patients missed by radiography (non-fractured) could potentially lose the opportunity for management, which could have contributed to the augmentation of their associated meniscal lesion symptoms that necessitated an MRI examination.

According to the MM classification, type I was diagnosed in 13 of our patients. Six patients were upgraded to grade II by MRI-based classification because these patients had a displacement of more than 2 mm at the anterior aspect of the avulsed fragment. One patient was upgraded to grade III by

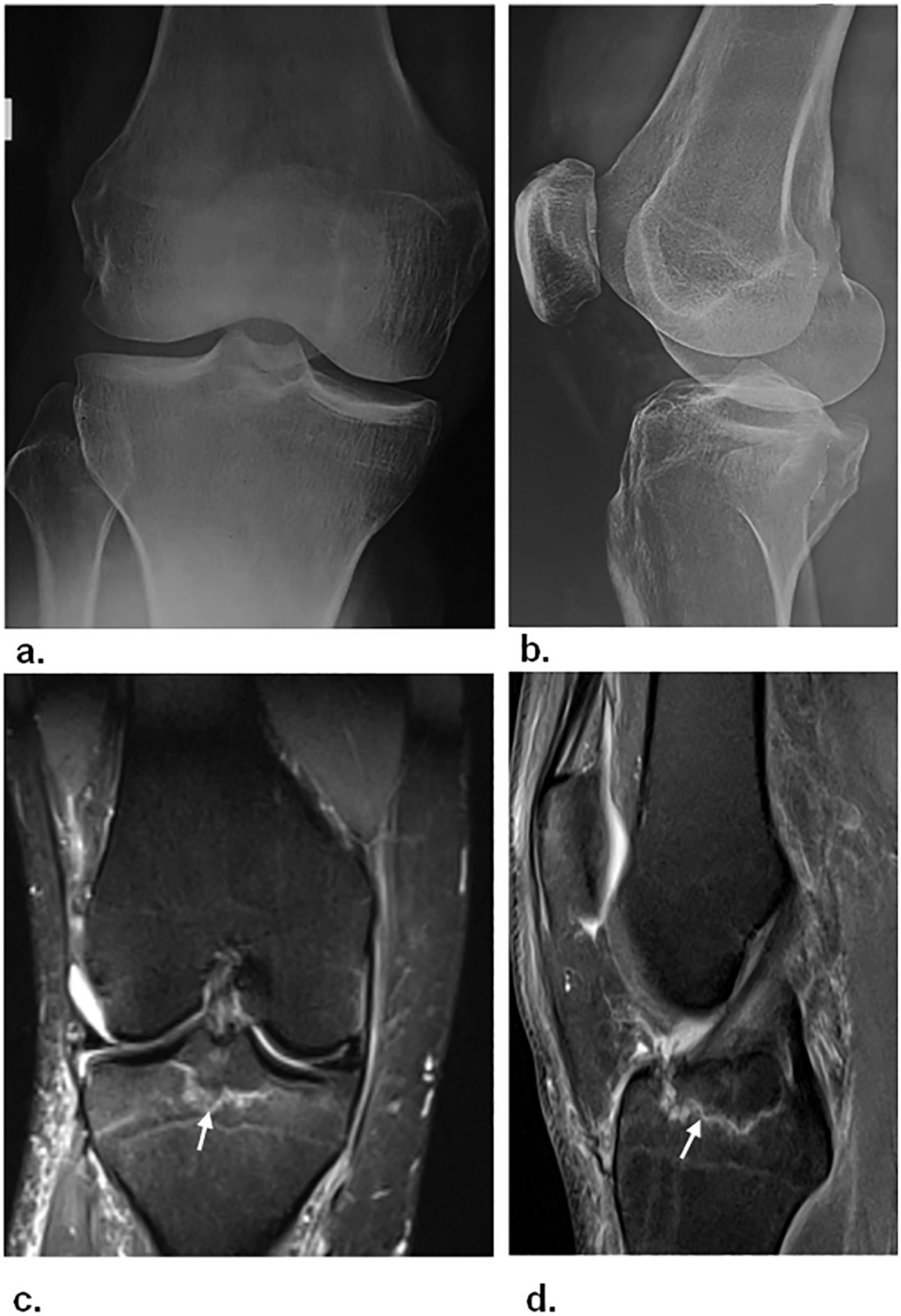

Figure 2. A 31-year-old male patient. (**a**) AP and (**b**) lateral views of plain radiography of the right knee shows no fracture lines. (**c**) Coronal STIR and (**d**) Sagittal PDFS reveals TSF (arrow) with < 2 mm displacement (grade I). AP, Anteroposterior; PDFS, proton density fat suppression; TSF, tibial spine fracture.

the MRI-based classification due to a displacement of > 2 mm at the posterior aspect of the avulsed fragment. One patient was downgraded to normal by the MRI-based classification due to the absence of the hypointense fracture line on T1WI and the edema on fluid-sensitive MRI sequences. 27 patients were classified as type II, according to the MM classification. Four patients were upgraded to grade III by MRI-based classification: two had meniscal entrapment, and two had > 2 mm displacement at the posterior aspect of the avulsed fragment. Three patients were downgraded to grade I by MRI-based classification because the avulsed fragment was posteriorly hung with < 2 mm displacement at the anterior aspect. 23 patients were classified as type III according to the MM classification. Four patients were

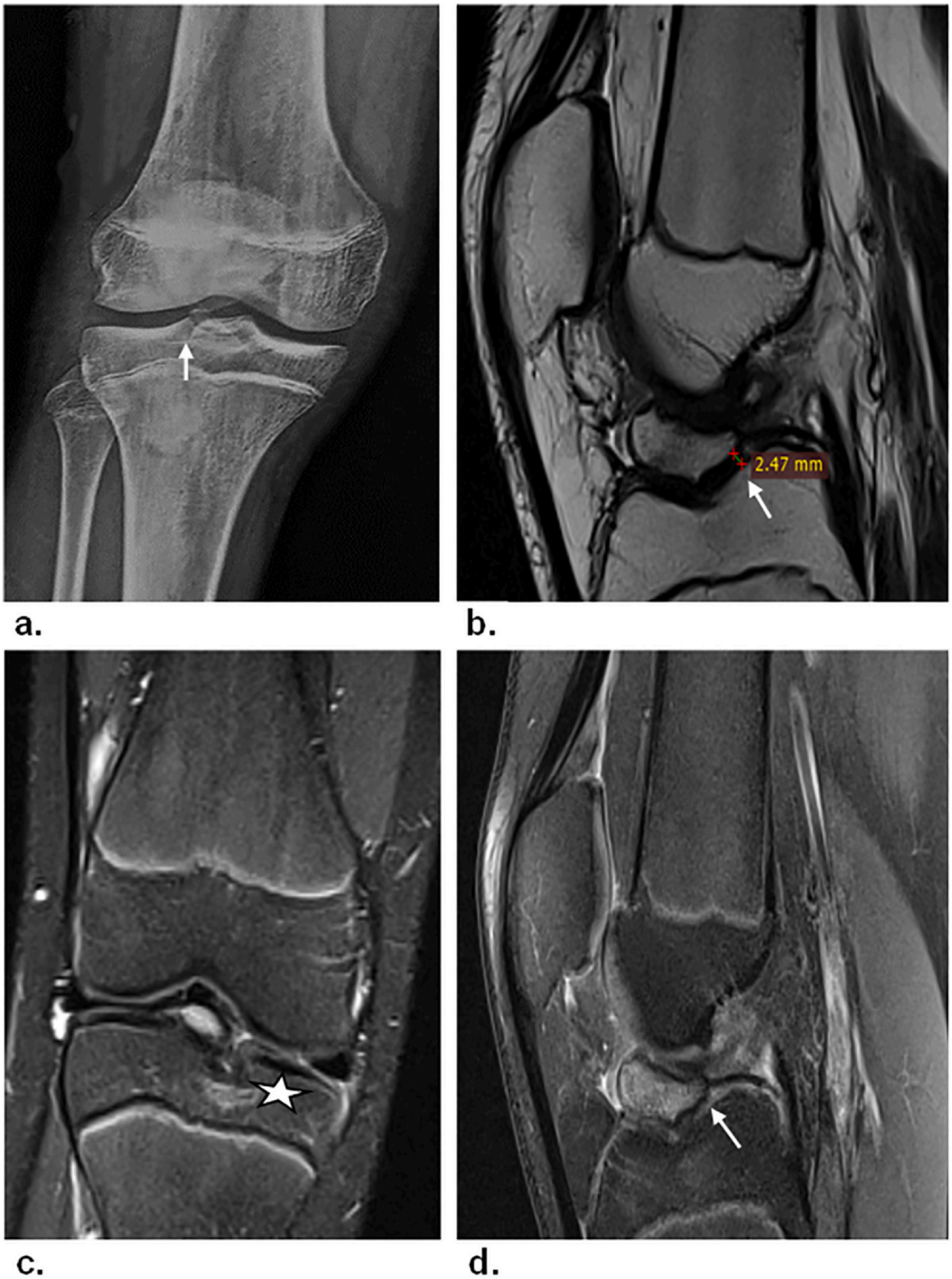

Figure 3. A 12-year-old male patient. (**a**) AP view of plain radiography of the right knee reveals TSF (arrow) with minimal displacement (Type II). (**b**) Sagittal T2WI, (**c**) Coronal STIR and (**d**) Sagittal PDFS reveals TSF (arrows) with > 2 mm posterior displacement with entrapped medial meniscus (*) (grade III). AP, Anteroposterior; STIR, short tau inversion recovery; PDFS, proton density fat suppression; TSF, tibial spine fracture.

downgraded to grade II based on the MRI classification. MRI revealed posterior-hinged fractures with > 2 mm displacement of the anterior aspect of the avulsed fragment in two patients and ≤ 2 mm displacement of the posterior aspect of the avulsed fragment in the other two patients. One potential advantage of MRI is the increasing number of TSF grade III cases. This increase in the determination of TSF grade III by MRI led to increased accuracy of the MRI-based classification. Specifying the grade of the fracture from II to III greatly influences the type of surgical intervention, as surgeons might prefer arthroscopy over open surgery and avoid the comorbidities encountered in open surgery.

Without stronger evidence for the reproducibility of the new MRI-based classification in the grading of TSFs, the results of the study become unusable in clinical practice, and it remains uncertain whether this classification should be used or not. In our study, we performed an inter-rater agreement analysis among three highly experienced radiologists. We found that the inter-rater reliability for grading TSFs was substantial for both the MM ($\kappa = 0.69$) and MRI-

Figure 4. A 24-year-old male patient. (**a**) AP and (**b**) lateral views of plain radiography of the right knee reveals TSF (arrow) with minimal displacement (Type II). (**c**) Coronal STIR and (**d**) Sagittal PDFS revealing TSF (arrows) with < 2 mm displacement (grade I).AP, Anteroposterior; PDFS, proton density fat suppression; TSF, tibial spine fracture.

based classifications ($\kappa = 0.79$). However, the use of MRI improved the inter-rater agreement among the three radiologists compared to plain radiographs. Our results are higher than those reported by Green et al. (17), who found that both MRI-based and MM classifications exhibited fair to moderate reliability ($\kappa = 0.38–0.66$). These higher values in our study may be explained by the higher experience of the radiologists. In contrast, Nguyen et al. (21) reported an almost perfect agreement in grading TSFs using conventional MRI ($\kappa = 0.92$); however, the sample size of their study was small. Our results also showed substantial agreement between the MM and MRI-based classifications regarding the grading of TSFs ($\kappa = 0.69$). Based on the substantial agreement among radiologists in our study, we recommend using the new MRI-based classification to improve diagnostic accuracy for grading TSFs.

We found that MRI has a potential role in detecting different associated soft tissue injuries with a detection accuracy of 89.7–94.1%, according to the radiologist. This finding was supported by a multicenter study conducted by Shimberg et al. (18), who observed a diagnostic accuracy of 92.7% for MRI for identifying concomitant injuries in TSFs.

In addition, Koon et al. (22) reported that MRI could be up to 95% accurate in identifying ACL tears. We detected partial ACL tears in 29.4% and complete ACL tears in 51.5% of the patients. Monto et al. (5) reported that intrasubstance or insertional ACL damage was found in 91% of patients.

Without pre-management MRI, meniscal tears can be clinically missed. Although meniscal tears without surgical intervention may heal spontaneously, others could develop mechanical instability (23). The current study found that meniscal lesions were among the most common soft tissue injuries in TSFs, accounting for 69.1% of patients. However, there were four false-negative cases with medial meniscal tears and three false-positive cases with lateral meniscal tears. These associated soft tissue injuries greatly impact the outcome of surgery, making it crucial to accurately diagnose and treat meniscal tears in patients with TSFs. It is important to develop better diagnostic tools and protocols to ensure that meniscal tears are not overlooked and that patients receive the appropriate treatment. A reliable classification system and evaluation of associated injuries are fundamental tools for appropriately managing TSFs (24).

Our study had certain limitations that need to be acknowledged. First, this was a monocentric retrospective study with a relatively small sample size. Further prospective research with larger sample sizes and multicenter designs may be needed to validate and generalize these findings. Second, the accuracy of the MRI-based classification was calculated only for TSFs with operative data, resulting in selection bias towards higher percentages of TSF grades II and III, which consequently impacted the diagnostic accuracy values. Third, all images were interpreted by highly experienced radiologists, which could have affected the diagnostic accuracy and explained the substantial inter-rater reliability. Therefore, further studies are required to assess the performance of this classification when applied by less-experienced radiologists. Fourth, the study did not evaluate the clinical outcomes of patients treated using the new MRI-based classification. Fifth, the study did not assess the cost-effectiveness of using MRI for all TSF grades, which may limit the feasibility of implementing the proposed system in some settings. Finally, MRI-based classification is not yet commonly used and may not be familiar to many clinicians.

CONCLUSION

The new MRI-based classification has proven to be a superior alternative to the MM classification as a diagnostic tool for grading TSFs. This is because of its higher detection efficacy, classification accuracy, and reliability as well as its ability to provide more comprehensive information about soft tissue injuries. However, it is important to note that while this new system shows promise, its wide adoption and acceptance within the medical community may require further validation studies and evidence of its clinical utility.

ETHICAL APPROVAL

Approval was obtained from the Institutional Review Board of Zagazig University in Egypt (approval number: ZU-IRB# 10739; approved on April 26, 2023).

FUNDING

This research was funded by the Deanship of Scientific Research, Najran University, Kingdom of Saudi Arabia, grant number NU/RG/MRC/12/1.

ETHICAL STATEMENT

This retrospective cross-sectional study was approved by the Institutional Review Board (approval number: ZU-IRB# 10739; approved on April 26, 2023). The requirement for written informed consent was waived due to the retrospective design of this study. All procedures were conducted in accordance with the principles of the Declaration of Helsinki.

CREDIT AUTHORSHIP CONTRIBUTION STATEMENT

Rania Mostafa Almolla, Hanan A. Hassan, Yassir Edrees Almalki, Maha Ibrahim Metwally, Mohamad Gamal Nada, and Mohammad Abd Alkhalik Basha designed the study and wrote the manuscript. All authors analyzed and interpreted the data and reviewed and approved the final version of the manuscript.

DATA AVAILABILITY

The datasets used and/or analyzed during the current study are available from the corresponding author on reasonable request.

DECLARATION OF COMPETING INTEREST

The authors of this manuscript declare no relevant conflicts of interest and no relationships with any companies whose products or services may be related to the subject matter of the article.

ACKNOWLEDGMENT

The authors are thankful to the Deanship of Scientific Research at Najran University for funding this work under the Research Groups Funding program grant code (NU/RG/MRC/12/1).

INFORMED CONSENT

Written informed consent was waived.

STATISTICS AND BIOMETRY

The corresponding author has great statistical expertise.

METHODOLOGY

- Retrospective.
- Diagnostic study.
- Performed at a single center.

REFERENCES

1. Fox JC, Saper MG. Arthroscopic suture fixation of comminuted tibial eminence fractures: hybrid all-epiphyseal bone tunnel and knotless anchor technique. Arthrosc Tech 2019; 8:e1283–e1288.
2. Ganley TJ, Brusalis CM. Surgical reduction and fixation of tibial spine fractures in children: multiple fixation strategies. JBJS Essent Surg Tech 2016; 6:e18.
3. Scrimshire AB, Gawad M, Davies R, et al. Management and outcomes of isolated paediatric tibial spine fractures. Injury 2018; 49:437–442.
4. Johnson AC, Wyatt JD, Treme G, et al. Incidence of associated knee injury in pediatric tibial eminence fractures. J Knee Surg 2014; 27:215–219.
5. Monto RR, Cameron-Donaldson ML, Close MA, et al. Magnetic resonance imaging in the evaluation of tibial eminence fractures in adults. J Knee Surg 2006; 19:187–190.
6. Gans I, Baldwin KD, Ganley TJ. Treatment and management outcomes of tibial eminence fractures in pediatric patients: a systematic review. Am J Sports Med 2014; 42:1743–1750.
7. Ishibashi Y, Tsuda E, Sasaki T, et al. Magnetic resonance imaging AIDS in detecting concomitant injuries in patients with tibial spine fractures. Clin Orthop Relat Res 2005; 434:207–212.
8. Horibe S, Shi K, Mitsuoka T, et al. Nonunited avulsion fractures of the intercondylar eminence of the tibia. Arthroscopy 2006; 16:757–762.
9. DeFroda SF, Hodax JD, Shah KN, et al. Tibial eminence fracture repair with double hewson suture passer technique. Arthrosc Tech 2017; 6:e1275–e1279.
10. Shin YW, Uppstrom TJ, Haskel JD, et al. The tibial eminence fracture in skeletally immature patients. Curr Opin Pediatr 2015; 27:50–70.
11. Meyers MH, Mckeever FM. Fracture of the intercondylar eminence of the tibia. J Bone Joint Surg Am 1959; 41:209–222.
12. Meyers MH, McKeever FM. Follow-up notes. Fracture of the intercondylar eminence of the tibia. J Bone Joint Surg Am 1970; 52:1677–1684.
13. Zaricznyj B. Avulsion fracture of the tibial eminence: treatment by open reduction and pinning. J Bone Joint Surg Am 1977; 59:1111–1114.
14. Feucht MJ, Brucker PU, Camathias C, et al. Meniscal injuries in children and adolescents undergoing surgical treatment for tibial eminence fractures. Knee Surg Sports Traumatol Arthrosc 2017; 25:445–453.
15. Ishibashi Y, Tsuda E, Sasaki T, et al. Magnetic resonance imaging AIDS in detecting concomitant injuries in patients with tibial spine fractures. Clin Orthop Relat Res 2005; 434:207–712.
16. Lafrance RM, Giordano B, Goldblatt J, et al. Pediatric tibial eminence fractures: evaluation and management. J Am Acad Orthop Surg 2010; 18:395–405.
17. Green D, Tuca M, Luderowski E, et al. A new, MRI-based classification system for tibial spine fractures changes clinical treatment recommendations when compared to Myers and Mckeever. Knee Surg Sports Traumatol Arthrosc 2019; 27:86–92.
18. Shimberg JL, Aoyama JT, Leska TM, et al. Tibial spine fractures: how much are we missing without pretreatment advanced imaging? a multicenter study. Am J Sports Med 2020; 48:3208–3213.
19. Zhang L, Xia Q, Yang R, et al. Anatomical factors associated with the development of anterior tibial spine fractures based on MRI measurements. J Orthop Surg Res 2023; 18:357.
20. Liu XD, Wang HB, Zhang TC, et al. Comparison between computed tomography and magnetic resonance imaging in clinical diagnosis and treatment of tibial platform fractures. World J Clin Cases 2020; 8:4067–4074.
21. Nguyen JC, Guariento A, Williams BA, et al. MRI evaluation of pediatric tibial eminence fractures: comparison between conventional and "CT-like" ultrashort echo time (UTE) images. Skeletal Radiol 2022; 51:1603–1610.
22. Koon D, Bassett F. Anterior cruciate ligament rupture. Southern Med J 2004; 97:755–756.
23. Song EK, Seon JK, Park SJ, et al. Clinical outcome of avulsion fracture of the anterior cruciate ligament between children and adults. J Pediatr Orthop 2009; 18:335–338.
24. Salvato D, Green DW, Accadbled F, et al. Tibial spine fractures: state of the art. J ISAKOS 2023. https://doi.org/10.1016/j.jisako.2023.06.001